Available online at www.sciencedirect.com
ScienceDirect
Journal of Molecular Catalysis A: Chemical 268 (2007) 155–162
JOURNAL OF MOLECULAR CATALYSIS A: CHEMICAL
www.elsevier.com/locate/molcata

Preparation of highly ordered Fe-SBA-15 by physical-vapor-infiltration and their application to liquid phase selective oxidation of styrene

Ling-Xia Zhang, Zi-Le Hua, Xiao-Ping Dong, Lei Li, Hang-Rong Chen, Jian-Lin Shi *

State Key Lab of High Performance and Superfine Microstructure, Shanghai Institute of Ceramics, Chinese Academy of Science, 1295 Ding-xi Road, Shanghai 200050, China

Received 15 November 2006; received in revised form 7 December 2006; accepted 10 December 2006
Available online 22 December 2006

Abstract

A simple physical-vapor-infiltration (PVI) method was applied to prepare highly ordered Fe-containing mesoporous silica SBA-15. The loading amount of Fe in SBA-15 was very high (up to 24 mol%) and can be tuned by using different PVI time. The liquid phase selective oxidation of styrene with H_2O_2 has been used to characterize their catalytic properties, the major product is benzaldehyde and the minor is styrene oxide. Independent of the Fe contents and the heat treatment temperature, the selectivity for benzaldehyde in the reaction at a mild temperature of 50 °C are all above 91%. At elevated temperature of 70 °C, the conversion rate of styrene increases beyond 36% and more significantly the selectivity for benzaldehyde can reach as high as 99%. Comparatively, another two different schemes (simple wet impregnation and incorporation using silane coupling agent) have been also applied to synthesize Fe-containing SBA-15 samples. Under the same condition, the styrene conversion on these two samples are both very low with minor product of phenylacetaldehyde and other styrene oxides.

Keywords: Mesoporous silica; Ferric oxides; Selective oxidation; Styrene; Hydrogen peroxide; Physical-vapor-infiltration

1. Introduction

Ordered mesoporous materials (OMMs) have been regarded as a perfect "natural microreactor", due to their highly ordered pore structure, high surface areas, narrow-distributed and tunable pore size. Inclusion chemistry of mesoporous materials has achieved great progresses for the construction of novel ordered and well dispersed nanocomposites with controlled size and size distribution [1a,2]. Mesostructured materials have attracted great research interests for their potential applications as catalysts, absorbents, chemical sensors and components in optical/electronic nanodevices, etc. Mesoporous silica are excellent hosts for various catalysts. Plenty of silanol groups make their modification more versatile and feasible. The controlled synthesis of nanostructured catalysts with high surface area and reproducible catalytic activity presents a great challenge [3]. It is a key object to keep the guest catalysts highly dispersed and narrow-sized in the mesoporous matrix and easily accessible to reactants. The introduction of metal nanoparticles for catalysis use has been centered on noble metal particles [1b,4,5]. Many oxide catalysts (*e.g.*, Fe_2O_3 [6,7], Ga_2O_3 [8], In_2O_3 [9], Cu_2O [10], TiO_2 [11], CeO_2 [12], ZrO_2 [13], etc.) have also been supported on the OMMs.

For supporting these guests in mesoporous materials, researchers have designed many different strategies, such as co-condensation, wetness impregnation, ion-exchanging, covalent bonding, surface modification, chemical vapor condensation, electrochemical condensation and supercritical fluids, ionic liquids as reaction media, etc. [1]. Different routes are suitable for different and/or specific kinds of guests to be incorporated into the pore channels, and different methods would lead to different existing states of guests. The metal or oxide guests are usually doped into the framework of OMMs by co-condensation and ion-exchanging processes. The covalent bonding and silane coupling routes commonly seem to form the oxide coatings on the pore surface at first. Many techniques such as selective modification of the outer pore surface, γ-irradiation and $scCO_2$ as reaction media, have been proved to be efficient in achieving narrow-size distribution and high dispersion control of the guest

* Corresponding author. Tel.: +86 21 52412712; Fax: +86 21 52413122/52413903.
E-mail address: jlshi@sunm.shcnc.sh.cn (J.-L. Shi).

1381-1169/$ – see front matter © 2006 Elsevier B.V. All rights reserved.
doi:10.1016/j.molcata.2006.12.027

nanomaterials. Electrodeposition and nanocasting techniques can give continuous nanowires/nanostructures, mainly for noble metal guests. The metal-organic chemical vapor infiltration (CVI) or deposition (CVD) method was developed to get Pd [14], GaAs [15], fullerene [16] and SiC [17] nanowires in mesoporous silica or nanostructures as a replica. The synthesis involves loading the organometallic precursor into template matrix via CVI or CVD, followed by mild thermal decomposition to generate Pd metal nanowires inside the template. Several special techniques, *e.g.*, *in situ* reduction at room temperature, template displacement, may lead to the formation of nanomaterials exclusively within the pore channels. The highly dispersive and narrow-sized guests in OMMs are especially favorable for catalytic applications if the pore structure still remains open for the easy access of reactants.

Benzaldehyde is a very important fine chemical product and can be widely used in many fields, such as medicine, dyes, flavors and resin additives. It is also a very important intermediate in the synthesis of other aroma compounds. The selective oxidation of styrene with H_2O_2 as oxidant to produce non-chlorine benzaldehyde was a green process. Most of the catalysts targeting this reaction are homogeneous noble metal-organic compounds [18,19]. There catalyst–product separation is a common problem. Therefore, research on heterogeneous catalysts become important and significant, and most of the studies have been focused on the molecular sieves (TS-1 [20], MCM-41and SBA-15 [21–23], etc.) incorporated with noble metals or transition metals. As above mentioned, transition metals introduction into mesoporous matrix have been frequently reported by direct hydrothermal treatment or impregnation method, etc. Catalytic activity for partial oxidation of hydrocarbons with H_2O_2 as oxidant in liquid phase reaction have also been studied by several groups [21–23]. Su and co-workers synthesized mono(V, Nb) and bimetallic (V or Nb–Ti, Ru–Cr, La–Mn, etc.) ions modified MCM-41 and found that these composites showed high catalytic activity in the selective oxidation of styrene by H_2O_2 [23]. Bao and Chen studied the catalytic activity of Ti-substituted SBA-15 in the selective oxidation of styrene [22].

Herein this report, a new simple physical-vapor-infiltration method is applied to prepare highly ordered Fe-containing mesoporous silica SBA-15, with an extraordinary high Fe loading amount up to 24 mol%. These composites were used to catalyze liquid phase selective oxidation of styrene with hydrogen peroxide as the oxygen source and exhibit a high selectivity for benzaldehyde.

2. Experimental

2.1. Synthesis

2.1.1. SBA-15

Mesoporous silica SBA-15 was synthesized according to a published procedure [24]. In a typical synthesis, 4 g of block copolymer surfactant $EO_{20}PO_{70}EO_{20}$ (Pluronic P123, BASF) was dissolved in 30 g of distilled water and 120 ml of 2 M HCl under stirring, followed by the addition of 8.5 g of tetraethyl orthosilicate (TEOS) at 35–40 °C. This gel was continuously stirred for 24 h and then crystallized in a Teflon-lined autoclave at 100 °C for 48 h. After crystallization, the solid product was filtered, washed with distilled water, and dried in air at 100 °C. The material was calcined in air at 530 °C for 6 h to remove the surfactant template and obtain a white parent powder (SBA-15).

2.1.2. Fe/SBA by PVI

The calcined SBA-15 and ferrocene were together put into a tightly sealed jar. Then the PVI process was carried out under 110 °C for different time periods (h: hours) and the obtained powder were finally calcined at 450, 550, and 750 °C in air. The composites were denoted as Fr-SBA-nh-T.

2.1.3. Fe/SBA by silane coupling

Fe-Ed-SBA-500 sample was synthesized in a similar way as reported before [25]. Amine functional groups were grafted onto the pore surfaces of mesoporous silica by refluxing the mixture of 1 g calcined SBA-15 and 5 ml *N*-[3-(trimethoxysilyl)-propylethylene]diamine (TPED) in 100 ml dry toluene under nitrogen atmosphere for at least 12 h. The resulting hybrid materials (denoted as ED-SBA-15) were filtered out using toluene and dried in vacuum.

One gram of $Fe(NO_3)_3{\cdot}9H_2O$ was dissolved in 50 ml dimethylformamide (DMF). Then 1 g of Ed-SBA-15 was added into the solution. After stirred for 24 h, the mixture was filtered and washed by DMF. Thus obtained powder was dried and calcined at 500 °C for 5 h in air and denoted as Fe-EdSBA-500.

2.1.4. MgFe/SBA and Fe/SBA by wet impregnation

To prepare MgFe/SBA sample, 1 g calcined SBA-15 was treated in vacuum at 300 °C and then was added into a ethanol solution of $Fe(NO_3)_3$ and $Mg(NO_3)_3$ (the mole ratio of Fe/Si and Mg/Si was 2% and 1%, respectively). For Fe/SBA synthesis, 3 mol% of Fe was added. After stirred for 24 h, the ethanol was evaporated at 50 °C under stirring. Thus obtained powder was dried and calcined at 500 °C for 5 h in air and denoted as MgFeSBA-500.

2.2. Characterization

XRD patterns were recorded on a Rigaku D/Max 2200PC diffractometer using Cu Kα radiation at 40 kV and 40 mA. Nitrogen adsorption/desorption isotherms at 77 K were measured on a Micromeritics TriStar 3000 instrument. All samples were outgassed at 200 °C for 12 h under flowing helium before the measurement. The specific surface areas were calculated with the BET (Brunauer–Emmet–Teller) methods. FETEM (Field Emission Transmission Electron Microscopy) analysis was conducted with a JEOL 200CX electron microscope operated at 200 keV. Energy dispersion spectrum (EDS) was obtained from an attached Oxford Link ISIS energy-dispersive spectrometer fixed on a JEM-2010 electron microscope operated at 200 kV. XPS (X-ray photoelectron spectroscopy) signals were collected on VG Micro MKII instrument using monochromatic Mg Kα X-ray at 1253.6 eV operated at 120 W. All the element binding energies were referenced to the C(1s) line situated at 284.6 eV.

2.3. Catalytic experiments

Styrene oxidation was carried out in a flask under stirring and refluxing as described in the literature [26]. Typically, 10 mmol styrene, 10 ml acetone, 0.1 g Fr-SBA-nh-T catalyst and 1.0 ml of 30 wt.% H_2O_2 were added successively into the flask. After 24 h reaction at 50 °C, the products were analysed with a gas chromatograph (GC–MS). The injector and colume temperature were 220 and 220 °C, respectively. *N*-Dodecane was used as an internal standard.

3. Results and discussion

3.1. XRD

Fig. 1 shows the XRD patterns of the samples. Small-angle XRD (SAXRD) pattern for the samples produced with different PVI time are listed in Fig. 1A. One major peak together with two additional peaks can be observed for samples with shorter time treatment. This is the characteristic hexagonal mesoporous structure of the SBA-15 matrix associated with *P6mm*. The three well-resolved peaks could be indexed as (1 0 0), (1 1 0) and (2 0 0) diffraction peaks. At longer PVI time, the loading amount of ferrocene became higher. The Fe introduction reduced the peak intensity of X-ray diffraction. However, the ferric oxide nanoparticles have an average diameter not larger than pore diameter of SBA-15 because no obvious signals for ferric oxide can be observed in their wide angel XRD (WAXRD) patterns (Fig. 1B), indicating that ferric oxide has been confined in pore channels independent of calcination temperature up to 750 °C (Fig. 1D). Calcination at higher temperature lead to higher X-ray diffraction intensity (Fig. 1C), which can be attributed to the densification of the ferric oxide nanoparticles on pore wall. Fe-EdSBA-500, FeSBA-500 and MgFeSBA-500 samples all have high intensity diffraction peaks (see Fig. 1C). This indicates that the highly ordered hexagonal mesopore structure have been well retained during the process using silane coupling agent and wet impregnation. And no peaks of crystalline ferric oxides

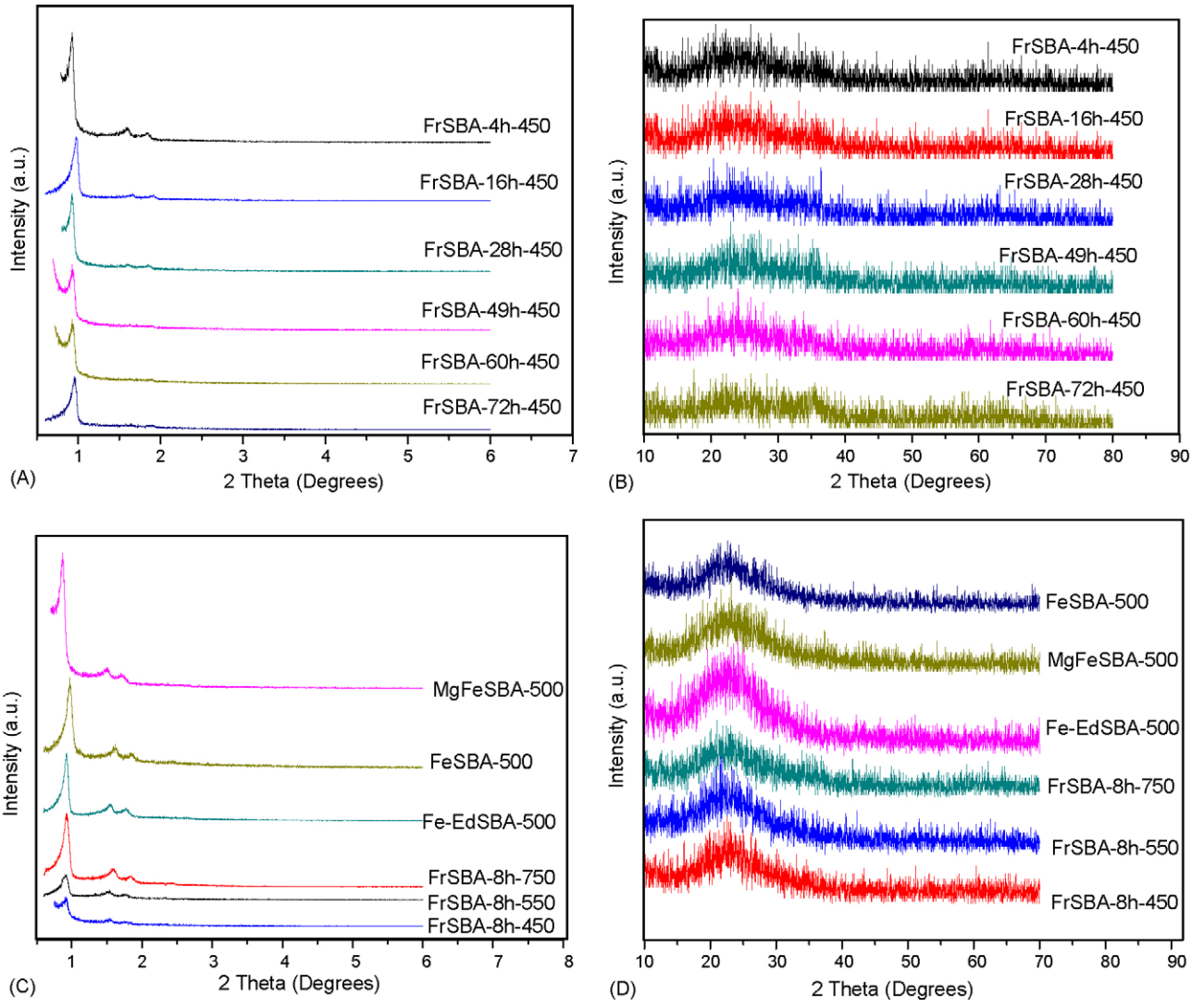

Fig. 1. XRD patterns of the samples.

can be identified. So metal oxide nanoparticles in these two samples have also been confined in the pore channels, which can be concluded from their WAXRD of these two samples (Fig. 1D).

3.2. TEM

During the preparation of catalysts, it is very important to keep the guest catalysts highly dispersed in pore channels of the mesoporous matrix and remain pore open to reactants. High resolution TEM images, as shown in Fig. 2, provide a direct observation of the highly ordered hexagonal mesoporous structure and the distribution of ferric oxide nanoparticles in the SBA-15 matrix. With the electron beam both parallel and perpendicular to the pore channels, no obvious bulk aggregates of the metal oxide on the outer surface could be found. These conclusions are in accordance with the SAXRD results. The simultaneous EDS analysis indicates the Fe exist inside the pore channels of SBA-15 (Fig. 2). EDS spectra collected from five differently elected regions gave similar results and an average Fe content is calculated to be as high as 24 mol% for FrSBA-72h-450 and 6.5 mol% for FrSBA-4h-450. The Fe nanoparticles introduced via this ferrocene PVI scheme should have been evenly confined in the pore channels of the mesoporous materials, and an open pore system of SBA-15 have been kept well after Fe introduction, as can be seen from the images and the pore size distribution (see Fig. 3). With the electron beam parallel to the pore channels, ferric oxide nanoparticles with diameters smaller than the pore size of SBA-15 matrix can be observed for samples prepared by longer time PVI. No nanowire can be observed in the pore channels.

3.3. N_2 sorption

The N_2 adsorption–desorption isotherms and pore distribution patterns for the samples, as shown in Figs. 3 and 4, gave

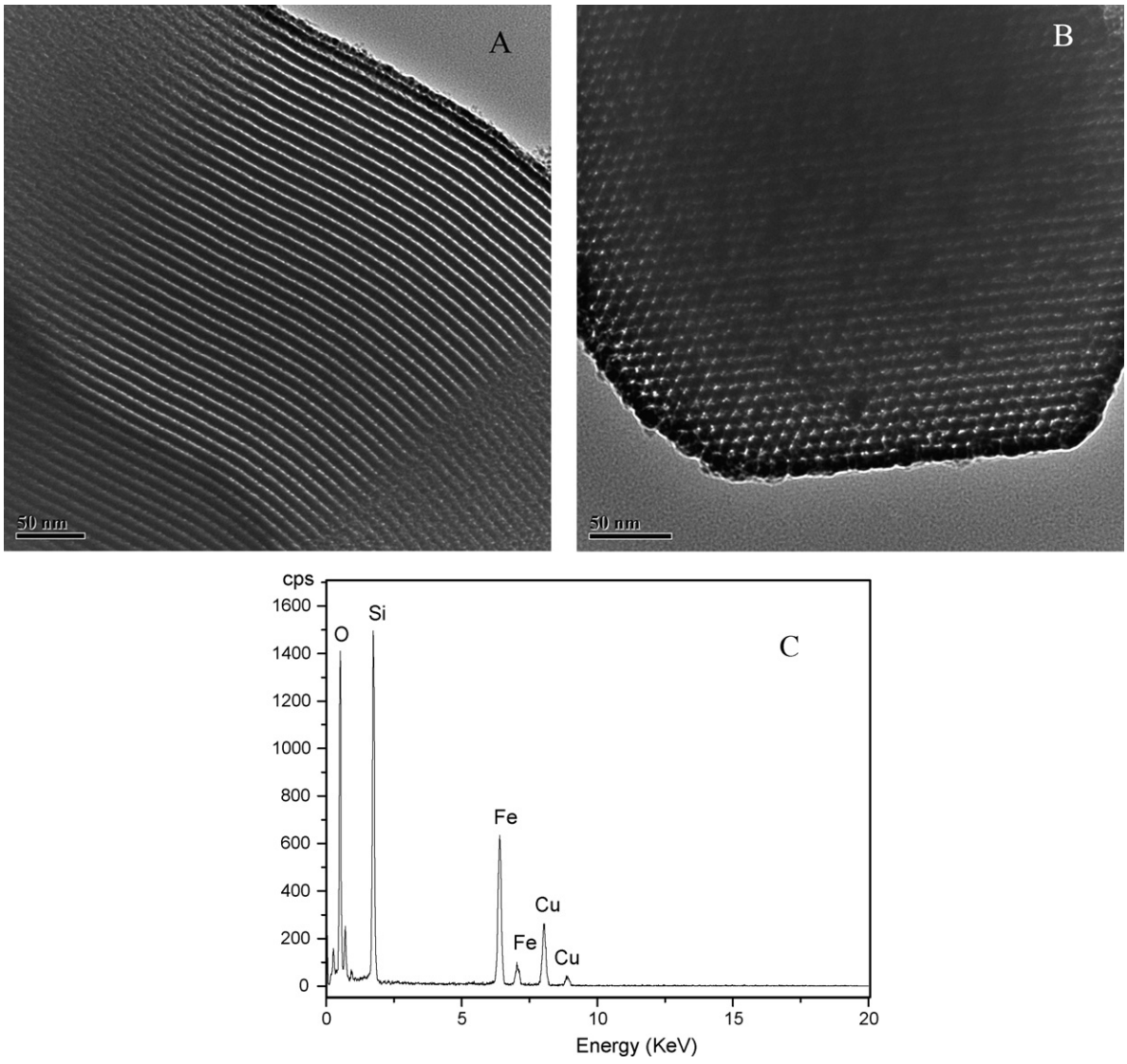

Fig. 2. High resolution TEM photos with the electron beam perpendicular (A) and parallel (B) to the pore channels and EDS spectrum (C) of the sample FrSBA-72h-450 collect from the former region.

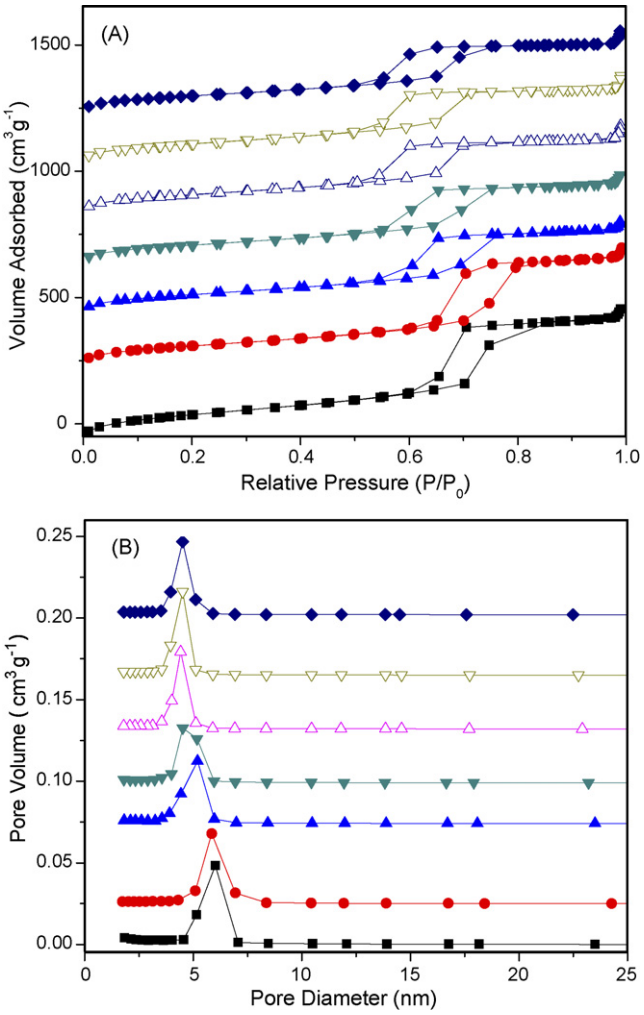

Fig. 3. The N_2 adsorption–desorption isotherms (A) and pore size distributions (B) of (■) calcined SBA-15, (●) FrSBA-4h-450, (▲) FrSBA-16h-450, (▼) FrSBA-28h-450, (△) FrSBA-49h-450, (▽) FrSBA-60h-450, (♦) FrSBA-72h-450.

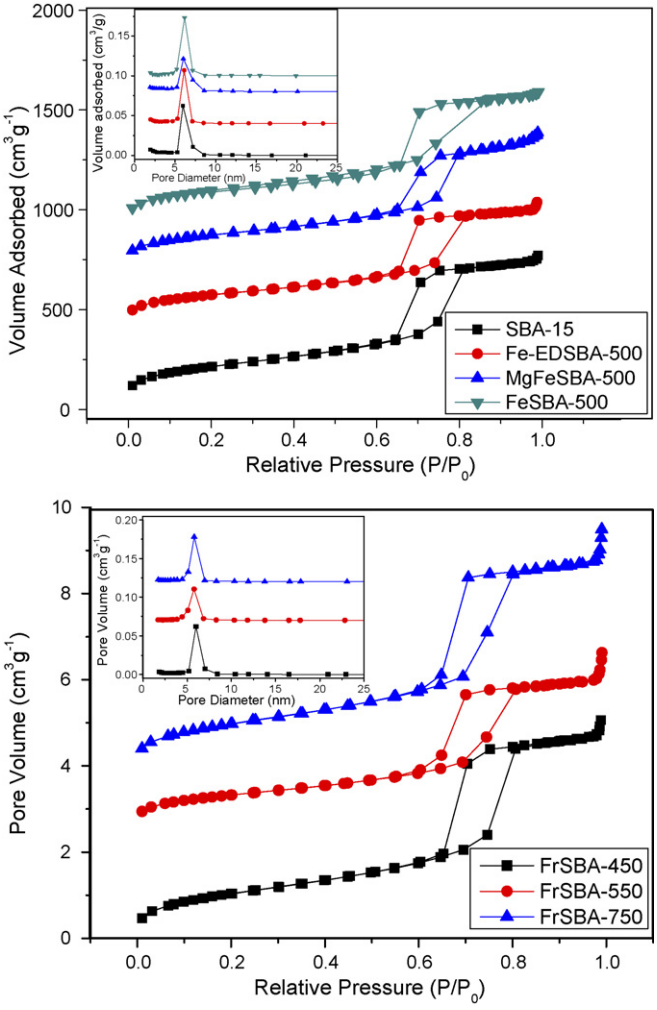

Fig. 4. Pore size distributions and the N_2 adsorption–desorption isotherms of samples Fe-EDSBA-500, MgFeSBA-500, FrSBA-T.

further details of their pore structure. The corresponding pore structural parameters are summarized in Table 1. Consistent with the above XRD and TEM analysis, all the samples have similar isotherm curves to that of SBA-15. Their irreversible type IV adsorption–desorption isotherms with a H1 hysteresis loop indicate their mesoporous channels and narrow pore size distributions. In each isotherm, the adsorption inflection at the relative pressure from 0.5 to 0.9 is associated with capillary condensation taking place in the mesopores and its steepness reveals the uniformity of mesopore size. The corresponding BJH desorption pore diameter distribution patterns show, with the PVI time became longer, their most concentrative pore diameter slightly shift to smaller size (Fig. 3). This indicates that the introduction of Fe into the mesopores have reduced their pore diameter, suggesting a type of the coating of ferric oxide nanoparticles on the inner pore surface of SBA-15. On the other hand, calcination at higher temperature bring no obvious change of their adsorption–desorption isotherms and their most concentrative pore diameters (Fig. 4), but a little larger average pore diameter

Table 1
Structure properties of the catalyst samples

Samples	BET surface area (m^2/g)	Pore diameter (nm)	Pore volume (cm^3/g)
SBA-15cal	775	6.8	1.20
MgFe-SBA-500	627	6.6	1.09
Fe-SBA-500	675	6.5	1.10
Fe-EdSBA-500	626	6.1	0.98
FrSBA-4h-450	530	6.0	0.90
FrSBA-8h-450	515	5.7	0.75
FrSBA-16h-450	402	5.6	0.64
FrSBA-28h-450	390	5.5	0.61
FrSBA-49h-450	389	5.2	0.61
FrSBA-60h-450	393	5.2	0.60
FrSBA-72h-450	357	5.3	0.57
FrSBA-8h-550	560	6.6	1.00
FrSBA-8h-750	539	7.2	1.08

as shown in Table 1. This could be related not only to the further polymerization and shrinkage of the silica framework, but also to densification of the ferric oxide coating on the pore surface. For Fe-EdSBA-500, FeSBA-500 and MgFeSBA-500 samples, their BET surface area and average diameters are both smaller than that of the parent SBA-15 because of the introduction of guest nanoparticles [25].

3.4. XPS

The presence of the ferric oxide nanoclusters inside the parent SBA-15 has also been detected by XPS. Fig. 5 shows the X-ray photoelectron spectra in the Fe $2p_{1/2}$ and $2P_{3/2}$, O 1s, Si 2s binding energy regions for FrSBA-4h-450 and FrSBA-72h-450 samples, respectively. The Fe $2p_{1/2}$ is centered at 723.8 eV and Fe $2p_{3/2}$ peak is centered at 710.3 eV. These match well with the Fe $2p_{1/2}$ and $2P_{3/2}$ in ferric oxide [27]. The intensity of these peaks is both heightened at longer PVI time to get more Fe loading in mesoporous silica SBA-15. This can also be revealed in the O 1s spectrum, which have been split into two peaks centered at 530.3 and 532.6 eV, corresponding to that in ferric oxide and silica, respectively. For the sample treated with 72 h PVI, the peak of 530.3 eV becomes much more intense than that of 4 h sample, leading to a much more obvious splitness of the O 1s peak. The same evidence can also been found from the intensity change of the peak of 103.0 eV in Si $2p_{3/2}$ spectrum.

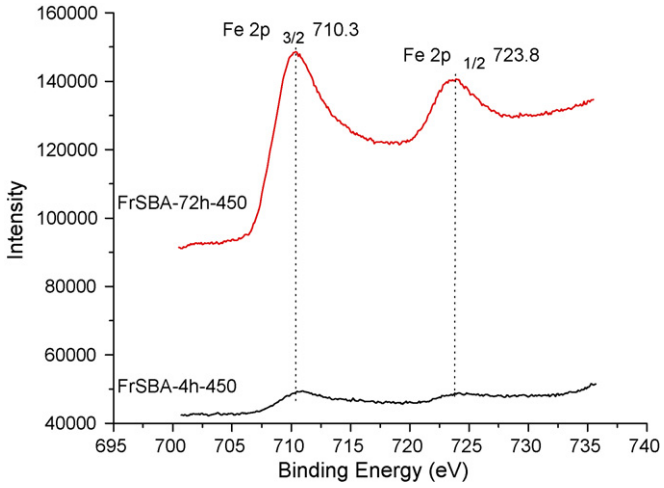

Fig. 5. XPS spectra of FrSBA-4h-450 and FrSBA-72h-450.

3.5. Catalytic activity in oxidation of styrene with H_2O_2

The catalytic results for the selective oxidation of styrene with H_2O_2 over the parent SBA-15 and all the Fe/SBA-15 samples are summarized in Table 2. As a blank experiment, calcined SBA-15 shows no catalytic activity towards the test reaction. The series of FrSBA-nh-T samples are all efficient catalysts for the selective oxidation of styrene with H_2O_2. The major product is benzaldehyde and the minor is styrene oxide. Independent of the

Table 2
Selective oxidation of styrene with H_2O_2 over the catalyst samples

Samples	Time (h)	Temperature (°C)	Styrene:H_2O_2 (molar ratio)	Styrene conversion (mol%)	Selectivity (mol%)		
					Benzaldehyde	Epoxide	Others[a]
SBA-15cal	24	50	1	–	–	–	–
MgFe-SBA-500	24	50	1	2.32	84.09	13.18	2.13
Fe-SBA-500	24	50	1	4.40	96.04	3.96	–
Fe-EdSBA-500	24	50	1	0.63	96.93	1.55	1.52
FrSBA-4h-450	24	50	1	6.45	94.29	5.71	–
FrSBA-8h-450	24	50	1	10.56	91.56	8.44	–
FrSBA-16h-450	24	50	1	11.21	91.69	8.31	–
	24	60	1	17.53	91.75	8.25	–
FrSBA-28h-450	16	50	1	10.50	87.81	13.52	-
	24	50	1	12.41	93.92	6.08	–
	48	50	1	14.41	90.32	9.68	–
	72	50	1	19.37	90.61	9.39	–
FrSBA-49h-450	24	50	1	11.40	91.80	8.20	–
	24	50	1/2	11.41	95.52	4.48	–
	24	70	1/3[a]	36.46	>99	–	–
FrSBA-60h-450	24	50	1	11.69	91.21	8.79	–
	3[b]	70	1	9.52	>99	–	-
FrSBA-72h-450	24	50	1	10.89	91.86	8.14	–
FrSBA-8h-550	24	50	1	7.548	93.41	6.59	–
FrSBA-8h-750	24	50	1	4.14	94.22	5.78	–

[a] Reaction conditions as same as Ref. [23]: cat., 70 mg; molar ratio styrene/acetone/H_2O_2 = 1/1.8/3; reaction temperature and time: 343 K and 24 h, respectively, in a glass flask reactor.

[b] Reaction conditions as same as Ref. [22]: cat., 300 mg; molar ratio styrene/H_2O_2 = 1/1; solvent, 10 ml CH_3CN; reaction temperature and time: 343 K and 3 h, respectively, in a glass flask reactor.

Fe content and the temperature of heat treatment, the selectivity for benzaldehyde are all above 91%, which is much higher than most of the mesoporous composites reported before [21–23]. In the oxidation of styrene during 24 h at a mild temperature of 50 °C, samples with PVI treatment time above 16 h show the similar conversion rates above 11%, with that of 28 h PVI treatment having the highest conversion of styrene. When the reaction temperature was raised to 70 °C, the conversion rate increase remarkably up to above 36% and more significantly, its selectivity for benzaldehyde can reach as high as 99%. Under the same reaction conditions as used in previous reports (see Table 2), these Fe/SBA-15 composites synthesized by PVI method show comparable conversion rate but much higher selectivity for benzaldehyde. In addition to elevated reaction temperature, reaction for longer reaction time can also increase the conversion of styrene.

The longer PVI time over 28 h in the preparation of the samples was not beneficial for the increase of styrene conversion and the selectivity of benzaldehyde, though a larger amount of Fe has been introduced into the mesoporous matrix. This could be attributed to the decrease of the BET surface and pore volume of the composites at higher Fe contents, which decreased the amount of the efficient active center and the accessibility of the catalyst sites for reactants. Higher temperature heat treatment for the samples at above 450 °C does not lead to higher conversion of styrene, probably due to the densification of the ferric oxide coating layer at higher temperature.

Comparatively, the selective oxidation of styrene with H_2O_2 over the Fe-SBA-500, MgFe-SBA-500 and Fe-EdSBA-500 samples show much lower conversion and small amount of phenylacetaldehyde and other styrene oxides have been yielded. For Fe-SBA-500 and MgFe-SBA-500, which were prepared by simple wet impregnation method, less loading amount (3 mol%) and lower dispersion of the metal oxides (i.e. pore blocking with metal oxides) may be responsible to their relatively poor catalytic activity. Although the application of silane coupling (Fe-EdSBA-500) have dramatically improved the dispersion of metal oxides and kept the pore channels unblocked, the least loading amount of the oxides (about 1.9 mol%) gave the lowest conversion of styrene (0.63%) as shown in Table 2. Herein this work, the PVI strategy have overcome these two drawbacks and brought us catalysts with both large loading amount and highly dispersion of metal oxides. Their much higher catalytic activity further indicates that the PVI scheme should be a more facile and efficient way to prepare ferric catalysts for selective oxidation of styrene with H_2O_2.

4. Conclusions

Herein this report, a new and simple physical-vapor-infiltration method has been developed to prepared highly ordered Fe-containing mesoporous silica SBA-15. The Fe content reached as high as 24 mol% and the highly ordered mesopore structure of SBA-15 can be well retained after PVI for 72 h. Limited effects of calcination and Fe loading on the mesoporous structure of the composites were found. The catalytic reaction of these mesoporous composites in the selective oxidation of styrene with H_2O_2 under mild conditions at 50 °C shows that the major product is benzaldehyde and the minor product is styrene oxide. Independent of the Fe content and the temperature of heat treatment, the selectivity for benzaldehyde in the reaction at 50 °C are all above 91%. At elevated temperature of 70 °C, the conversion rate increases beyond 36% and more significantly the selectivity for benzaldehyde can reach as high as 99%. Fe-containing SBA-15 samples prepared by another two schemes using silane coupling agent and simple wet impregnation gives much lower conversation of styrene with small amount of other byproducts (such as phenylacetaldehyde and other styrene oxides). This indicates that the PVI scheme should be a facile and efficient way to prepare this kind of catalysts for highly selective oxidation of styrene with H_2O_2.

Acknowledgements

The authors gratefully acknowledge the financial supports from the National Science Foundation of China (Grant Nos. 20633090, 50672115), the Shanghai Science and Technology Committee (Grant Nos. 0452nm056, 0652nm014, 06ZR14163, 06DZ05116).

References

[1] (a) J.L. Shi, Z.L. Hua, L.X. Zhang, J. Mater. Chem. 14 (2004) 795; (b) L.X. Zhang, J.L. Shi, J. Yu, Z.L. Hua, X.G. Zhao, M.L. Ruan, Adv. Mater. 14 (2002) 1510.
[2] L. Li, J.L. Shi, Chin. J. Catal. 26 (2005) 159.
[3] T. Bell, D.M. Antonelli, Adv. Mater. 10 (1998) 846.
[4] P. Mukherjee, C.R. Patra, A. Ghosh, R. Kumar, M. Sastry, Chem. Mater. 14 (2002) 1678.
[5] Y. Nishihata, J. Mizuki, T. Akao, H. Tanaka, M. Uenishi, M. Kimura, T. Okamoto, N. Hamada, Nature 418 (2002) 164.
[6] M. Iwamoto, T. Abe, Y. Tachibana, J. Mol. Catal. A 155 (2000) 143.
[7] C. Garcia, Y. Zhang, F. DiSalvo, U. Wiesner, Angew. Chem. Int. Ed. 42 (2003) 1526.
[8] V.R. Choudhary, S.K. Jana, B.P. Kiran, J. Catal. 192 (2000) 257.
[9] H. Yang, Q. Shi, B. Tian, Q. Lu, F. Gao, S. Xie, J. Fan, C. Yu, B. Tu, D. Zhao, J. Am. Chem. Soc. 125 (2003) 4672.
[10] A. Zecchina, D. Scarano, G. Spoto, S. Bodiga, C. Lamberti, G. Bellussi, Stud. Surf. Sci. Catal. 117 (1998) 343.
[11] S. Zheng, L. Gao, Q.H. Zhang, W.P. Zhang, J.K. Guo, J. Mater. Chem. 11 (2001) 578.
[12] K. Kloetstra, H. van Bekkum, Stud. Surf. Sci. Catal. 105 (1997) 431.
[13] W.H. Zhang, J.L. Shi, L.Z. Wang, D.S. Yan, Mater. Lett. 46 (2000) 35.
[14] K.B. Lee, S.M. Lee, J. Cheon, Adv. Mater. 13 (2001) 517.
[15] H. Parala, H. Winkler, M. Kolbe, A. Wohlfart, R.A. Fischer, R. Schmechel, H. Seggern, Adv. Mater. 12 (2000) 1050.
[16] B. Ye, M. Trudeau, D. Antonelli, Adv. Mater. 13 (2001) 561.
[17] P. Krawiec, C. Weidenthaler, S. Kaskel, Chem. Mater. 16 (2004) 2869.
[18] A.S. Kanmani, S. Vancheesan, J. Mol. Catal. A 150 (1999) 95.
[19] A.M. Al-Ajiouni, J.H. Espenson, J. Am. Chem. Soc. 117 (1995) 9243.
[20] S.B. Kumar, S.P. Mirajkar, G.C.G. Paris, P. Kumar, R. Kumar, J. Catal. 156 (1995) 163.
[21] Y. Luo, J. Lin, Microporous Mesoporous Mater. 86 (2005) 23.

[22] Y.Y. Chen, Y.L. Huang, J.H. Xiu, X.W. Han, X.H. Bao, Appl. Catal. A: Gen. 273 (2004) 185.
[23] V. Părvulescu, C. Anastasescu, B.L. Su, J. Mol. Catal. A: Chem. 198 (2003) 249.
[24] D.Y. Zhao, Q.S. Huo, J. Feng, B.F. Chemlka, G.D. Stucky, J. Am. Chem. Soc. 120 (1998) 6024.
[25] W.H. Zhang, J.L. Shi, H.R. Chen, Chem. Mater. 13 (2001) 648.
[26] N. Ma, Y.H. Yue, W.M. Hua, Z. Gao, Appl. Catal. A: Gen. 251 (2003) 39.
[27] B.J. Tan, K.J. Klabunde, P.M.A. Sherwood, Chem. Mater. 2 (1990) 186.